NAWCWPNS TP 8036

Molecular Modeling Study on the Mechanical Properties of Polybenzimidazole

by
Nancy E. Iwamoto
Research Department

JULY 1992

NAVAL AIR WARFARE CENTER WEAPONS DIVISION
CHINA LAKE, CA 93555-6001

Naval Air Warfare Center Weapons Division

FOREWORD

This report documents computer modeling studies done at the Naval Air Warfare Center Weapons Division, China Lake, Calif., in support of basic research of the environmental effects on composite polymer binders, begun in FY90 and finished in FY92. The purpose of this work was to examine and document the feasibility of using molecular mechanics and dynamics as a predictive tool for the affects of structure on the mechanical responses in polymer systems. This project was funded by the Office of Naval Research.

This report has been reviewed for technical accuracy by Geoffrey A. Lindsay.

Approved by
R. L. DERR, *Head*
Research Department
30 June 1992

Under authority of
W. E. NEWMAN
RAdm., U.S. Navy
Commander

Released for publication by
W. B. PORTER
Deputy Commander for Research & Development

NAWCWPNS Technical Publication 8036

Published by ..... Technical Information Department
Collation ..... Cover, 18 leaves
First printing ..... 55 copies

DEPARTMENT OF THE NAVY
NAVAL AIR WARFARE CENTER
WEAPONS DIVISION
CHINA LAKE, CALIFORNIA 93555-6001

IN REPLY REFER TO:
5600
Ser 8966
9 Sep 92

MEMORANDUM

From: Commander, Naval Air Warfare Center Weapons Division
To: Distribution

Subj: ERRATA FOR NAWCWPNS TECHNICAL PUBLICATION 8036, *MOLECULAR MODELING STUDY ON THE MECHANICAL PROPERTIES OF POLYBENZIMIDAZOLE,* Dated Jul 92

1. Please make the following pen and ink changes on the subject report: Page 12, Figure 1 legend, change the first word, "Top:" to "Bottom" and the sixth word, "Bottom:" to "Top".

B. W. BUTLER
By direction

REPORT DOCUMENTATION PAGE

Form Approved
OMB No. 0704-0188

1. AGENCY USE ONLY *(Leave blank)*	2. REPORT DATE	3. REPORT TYPE AND DATES COVERED
	July 1992	Final Dec 89-Mar 92

4. TITLE AND SUBTITLE
Molecular Modeling Study on the Mechanical Properties of Polybenzimidazole

5. FUNDING NUMBERS
Task ROONO
Program 1117 14
Element 61152N

6. AUTHORS

Nancy E. Iwamoto

7. PERFORMING ORGANIZATION NAME(S) AND ADDRESS(ES)

Naval Air Warfare Center Weapons Division
China Lake, CA 93555-6001

8. PERFORMING ORGANIZATION REPORT NUMBER

NAWCWPNS TP 8036

9. SPONSORING/MONITORING AGENCY NAMES(S) AND ADDRESS(ES)

Office of Naval Research
800 North Quincy Street
Arlington, VA 22217-5000

10. SPONSORING/MONITORING AGENCY REPORT NUMBER

11. SUPPLEMENTARY NOTES

12a. DISTRIBUTION /AVAILABILITY STATEMENT

Approved for public release; distribution is unlimited.

12b. DISTRIBUTION CODE

13. ABSTRACT *(Maximum 200 words)*

The effects of molecular structure on the mechanical properties of a polymer system has long been of interest to polymer chemists, physicists, and engineers. Much work has been done in mechanical modeling and in statistical mechanics to describe the working polymer. With the advent of molecular mechanics and dynamics and the general use of Newtonian techniques, an added dimension is available to study structural effects on the inter- and intramolecular level that may directly contribute to mechanical behavior. In this study, molecular modeling has been used in order to understand the water absorption characteristics of polybenzimidazole (PBI) and its effect on mechanical properties.

14. SUBJECT TERMS
Polybenzimidazole, Molecular modeling, Structure-property correlations, Mechanical behavior, Water affinity, Hydrogen bonding tendencies

15. NUMBER OF PAGES
34

16. PRICE CODE

17. SECURITY CLASSIFICATION OF REPORT	18. SECURITY CLASSIFICATION OF THIS PAGE	19. SECURITY CLASSIFICATION OF ABSTRACT	20. LIMITATION OF ABSTRACT
UNCLASSIFIED	UNCLASSIFIED	UNCLASSIFIED	UL

CONTENTS

INTRODUCTION

At the Naval Air Warfare Center Weapons Division (NAWCWPNS), a Newtonian molecular mechanics and dynamics model is being used to help understand and predict underlying correlations between molecular structure and mechanical behavior in polymeric systems.

Molecular mechanics and dynamics is a Newtonian-based calculation that uses force-field parameterization of the atom and bond types integrated into an expression to define the potential energy of a molecule or molecular system (Reference 1).

E = bond stretch + bend angles + torsion + out of plane +
cross terms + (coulombic, electrostatic)

General static molecular conformations are generated using energy minimization methodology that searches for energy minima whereas dynamics methodology is used to explore effects of temperature and/or external forcing on the system.

As a demonstration of the usefulness of this tool, the model was applied in a hydration study of polybenzimidazole (PBI). PBI is a highly amorphous polymer with fused aromatic ring structure. Because of its exceptionally high thermal stability, PBI is of interest as a component in high-temperature stable composite materials and fibers. However, PBI absorbs water up to 18% by weight which also degrades the stiffness and strength properties of the material. Stabilization of the hydration characteristics of the material would be desirable in order to stabilize the mechanical properties. Although hydration studies of PBI have been performed in the past (References 2 through 9), mechanistic studies which relate the impact of molecular structure on mechanical properties have not been widely studied (References 8 through 10).

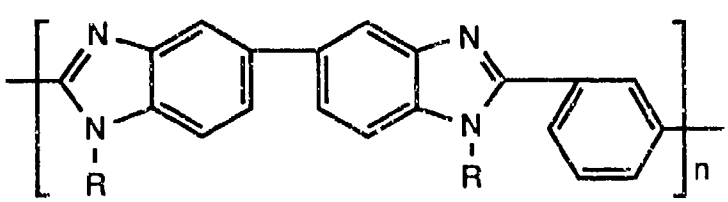

Molecular modeling was first applied to predict water affinity characteristics of PBI and the effects of simple substitution. The model was then extended to study small strain stiffness characteristics upon hydration and further expanded to include a suggested method in which to study failure tendencies.

A standard commercial molecular modeling package (obtained from Biosym Technologies, Inc., San Diego, Calif.) was used throughout this study in order to explore the feasibility of using Newtonian techniques to model mechanical properties on the molecular level.

RESULTS AND DISCUSSION

For most of the calculations, a small system consisting of two trimer strands of PBI were used in order to help minimize processing time. Both strands were initially oriented in order to approximate PBI in its strongest form of interest for fibers and composites. Upon minimization, the two stranded model formed an intertwined helix (Figure 1). Although the polymer was initially constructed in an oriented fashion, there appeared to be no obvious intramolecular or inter-chain hydrogen bond stabilization to the system, although there are experimental reports of hydrogen bonding in PBI (References 5 through 7). Lack of such stabilization would help to explain amorphous formation in the polymer, since there would be no overriding factors which would favor auto-alignment or orientation. In addition, the helical nature of the minimized structure suggested that the amorphous nature of PBI could also arise from interruption of any long-term periodicity needed for crystallinity by independent skewing of the polymer axis.

HYDRATION TENDENCIES

In order to study hydration tendencies, both strands of PBI were surrounded by a 5 angstrom layer of water and the system brought to an energy minimum. The amount of moisture affinity was predicted by calculating the number of water molecules equilibrated within hydrogen bonding distance. For unsubstituted PBI, the model predicted 23 water molecules hydrogen bonded to the amine and imine nitrogens of PBI. This prediction is in agreement with the 15-18% by weight seen experimentally.

The model was extended to substituted systems by replacing the amine hydrogen with hydrophobic groups such as ethyl, butyl, t-butyl and phenyl. In each case the substituted groups were placed on the same sides of both chains. Each sample was minimized with a 5-angstrom layer of water and again moisture affinity predicted by calculating the number of water molecules equilibrated within hydrogen-bonding distance (Figure 2). In each case the amount of water that was hydrogen-bonded to PBI dropped by approximately one-half. Upon examination, the origin of this drop stemmed from exclusion of water from the substituted side of the polymer (Figure 3). Water exclusion by both substitution and regiochemistry indicated that simple substitution will aid in resisting moisture uptake by loss of the availability of a labile hydrogen, but will not completely eliminate the tendency toward hydration. Interestingly, size of the hydrocarbon group had a negligible impact on the water affinity, indicating a negligible steric contribution to hydration tendencies from the side group.

The model was briefly repeated with only the ethyl and t-butyl cases, this time with substitution on opposite sides of the respective chains in order to test sensitivity for regiochemistry. The relative placement of groups is shown below for an example. In both instances, the amount of hydrogen bonded water molecules slightly increased. The increase occurred mainly on the imine side of the chains. The ethyl model had the greatest difference from the original, increasing in hydration by about 67% between substitution on the same side versus opposite sides of the chains. The t-butyl model increased hydration by only 9%. However, the average hydration and the general trend remained similar (Figure 4) to the previous models, which may be a better representation.

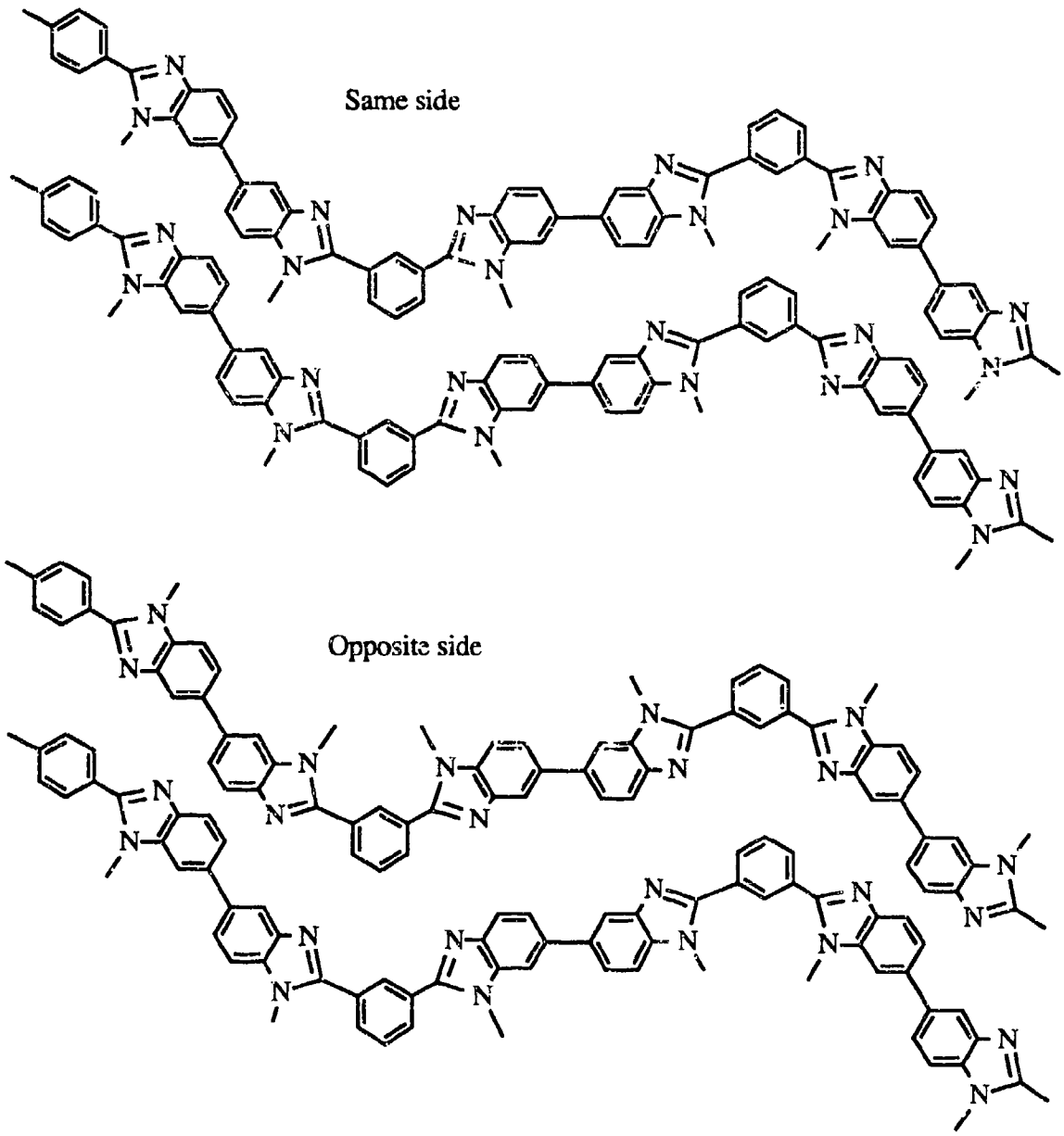

MECHANICAL PROPERTIES

Dynamics modeling was also used in order to predict stiffness trends or characteristics. The dynamics were accomplished first by equilibrating the hydrated (5-angstrom layer, >75% water) minimized structure at room temperature, then imposing a forcing potential along the axis of the two strands, in effect shearing the strands apart along the axis (Figure 1). The energy profiles obtained are shown in Figure 5. This process was repeated with varying amounts of hydration. Lower hydration levels were obtained by eliminating water molecules beyond hydrogen-bond distances, and then systematically reducing the amount of water in the system. This produced models with approximately 20

and 10% hydration (Figure 6). The model was also repeated by equilibrating varying thicknesses of water around the trimers. Both hydration methods exhibited the same general trends.

The most obvious trend occurred at the beginning of the stress trajectories. In each case, the initial energy barrier to the induced stress in the unhydrated case was diminished upon hydration, suggesting a source of the mechanical softening effect by water. The effect of water on the energy barrier was especially noticeable in the >75% hydrated case where the barrier to stress disappeared (Figure 6). Initial slopes were calculated as a quantitative indication of stiffness trends, or change in energy with strain, upon hydration (see Figure 7, Trimers Crude). The models were repeated with a refinement using smaller steps. The initial slopes calculated from the refined cases were found to be in agreement with published modulus trends (References 2 through 4) with hydration (normalized at an extrapolated unhydrated modulus) (Figure 7).

Since the actual material will undergo different types of stress interactions, the forcing potential was imposed in a second direction in the middle of both strands perpendicular to the axis (Figure 8) using similar pull rates (as defined by distance/time at approximately 12-13 angstroms/picosecond). For this rate, the relative initial slopes for the perpendicular direction were comparable to the axial direction. As expected from the axial case, the initial slopes decreased with increasing hydration so there were no improvements in the resistance to strain with hydration in this stress direction.

In all cases whether using an axial or perpendicular stress, a similar trend occurred in the energy curves: as hydration increased, the initial energy barrier both decreased and shifted to lower strain. These trends arising from hydration could effectively decrease initial slopes or stiffness and decrease the strength of the material.

The rate dependencies were further considered by repeating the axial and perpendicular energy profiles at the same strain rate defined by strain/time. This method was considered to be a more realistic rate comparison than using absolute rates of distance/time, because of the differing initial dimensions used. In this case, the lowest rates studied for the axial and perpendicular directions were compared at 12 (Figure 6) and approximately 2 angstroms/picosecond (Figure 9) respectively, both of which convert to approximately 0.4 ps^{-1} using the adjusted rate definition of strain/time. As expected by less intermolecular contact and thus lower intermolecular contributions to the total energy for the perpendicular direction, the energy barrier to strain was decreased in the perpendicular direction from that of the axial strain direction. This decrease suggested that axial stress orientation (rather than perpendicular) could be a major contributor to the modulus or stiffness of the polymer. Also for the perpendicular stress, the energy progression with strain became more random and scattered. This scatter was especially noticeable in the hydrated states in which the barrier to strain completely disappeared, with no initial slope. The more random scatter of energy with strain suggested that contributions from both the perpendicular strain direction, as well as from hydration, may lead to sufficient energetics encouraging the polymer to flow (i.e., no internal resistance to the strain imposed). For example, in a matrix consisting of both perpendicular and axial strain (especially hydrated), flow could occur primarily from the perpendicular orientation and stress may build primarily as a result of the axial orientation with its high barrier to strain at all hydrations. At low hydration concentrations, a stress could result from a combination of both contributions, with the axial orientation contributing the most to the strength of the material.

The trends following stiffness or modulus were also examined by comparing the data from the model with the experimental changes in modulus with draw ratio (Reference 2). Assuming that the undrawn state is related to the perpendicular stress direction and that the drawn state is related to the axial stress direction, the relative modulus (the undrawn to the drawn experimental modulus ratio) and the relative initial slopes of the energy profiles from perpendicular to parallel stresses were compared. These results are represented in Figure 10, which plots orientation (1 = axial or drawn, 0 = perpendicular or undrawn) with relative modulus. Similar strain rates were used for the relative modulus calculations of the model data (at both 0.4 ps^{-1} and approximately 1 ps^{-1}. Although other possible strain directions have not yet been included in the study, the trends are similar to experimental, and the range in the model results were in agreement with expected ratios in modulus. As previously mentioned, scatter in the model data at the low perpendicular strain rates would help to explain deviations from experimental

In order to further investigate rate dependencies, the perpendicular stress models were rerun at an intermediate strain rate (5-7 angstroms/ps or approximately 1 ps^{-1}) by changing the forcing potential (Figure 11), and compared with the high and low strain rates already determined. The progression of the trends with rate was consistent. The energy barriers to strain generally decreased with decreasing rate and with increasing hydration. For the highly hydrated cases the initial energy barrier disappeared, indicating a tendency to flow. And as previously mentioned, at the lowest strain rates the points defining the energy progression with strain became more scattered. This increase in scatter may be especially important since energetically the molecule has less defined energy differences to strain and so has an adequate pathway for flow to occur. Because the loss of the energy barrier and the increase in scatter are both consistent trends with rate, such trends may suggest an available method in which to molecularly study rate processes such as creep, stress relaxation, and normal strain response. (However, such trend analysis is only a suggestion since scaling factors between the molecular and bulk processes have not yet been considered and must be another topic of study. Also note that in the present study only trends were considered instead of absolute measures.) These rate trends are summarized in Table 1.

The axial stress model was rerun only once at a slightly higher rate (Figure 12). At this rate all of the curves at each hydration level appear to be comparable, or are approaching comparability. Such leveling of the energy curve trends with rate may be expected on the basis of time-temperature superposition. These general trends suggest that it may be possible in the future to predict master curves, given that the specific interactions and contributions are adequately modeled and understood.

Interestingly, several other trends in the energy profiles with hydration followed mechanical property trends of the material. The experimental strain-to-break and tensile strength both decrease with increasing hydration. In order to analyze these trends, the failure point was arbitrarily defined from the energy profiles at the strain level in which the total energy of the system dropped below its initial energy. The tensile strength was also arbitrarily defined by the change in energy from initial energy to energy at the curve break point or the point at which the energy apparently maximized or began to level. (This break point could also indicate yield, but more work will have to be done to clarify the significance of the break point, as well as the locations of expected failure.) It was found that both the strain and energy difference at the defined failure points decrease with increasing hydration in both strain types (axial and perpendicular) (Figure 13). As seen in

Figure 13, the qualitative trend is in agreement with experimental trends. Using the same strain rate in order to compare the axial to the perpendicular cases, the quantitative trends appear to have a closer correlation for the axial direction at the lower 0.35 ps^{-1} data, since the perpendicular direction loses its barrier to strain upon hydration. This correlation suggests that the more important contribution for strength or toughness may stem from the axial orientation (of course, the relative importance of contributions from the different orientations have not been vigorously studied in this analysis). With higher rates such as at 0.9-1.3 ps^{-1}, the trends for the axial direction become hydration independent (Table 1), but appear comparable to experimental from the perpendicular stress direction especially at strain-to-break (Figure 13). This suggests an added concern over the effect of rate dependencies upon failure mechanisms. Generally, however, the trend in the perpendicular case is similar to that of the axial case in that an increase in hydration resulted in a decrease in initial slope or stiffness (modulus), a decrease in the defined change in energy (strength) and a decrease in the defined change in dimension at failure (strain-to-break).

TABLE 1. Rate and Orientational Effects.

Stress	Hydration	Speed, Å/ps	Strain rate, ps^{-1}	Approximate slope
Axial	0	12	0.35	35
Axial	10.5	12	0.35	19
Axial	20	12	0.34	11
Axial	0	28	0.81	90
Axial	10.5	30	0.88	95
Axial	20	28	0.78	85
Axial	20	24	0.67	75
Perpendicular	0	13	2.5	32
Perpendicular	10.5	13	2.6	27
Perpendicular	20	13	2.9	12
Perpendicular	0	7	1.3	17
Perpendicular	10.5	5	1.0	25
Perpendicular	20	6	1.3	0
Perpendicular	0	2.2	0.43	17
Perpendicular	10.5	1.6	0.31	0
Perpendicular	20	1.8	0.4	0

Stiffness trends for the substituted cases were also briefly investigated in order to gauge the impact of substitution and hydration. For each substituted polymer, the forcing potentials were used in the axial direction on the unhydrated and hydrated (>75% water) cases, and in the perpendicular direction only for the unhydrated model as a comparison against the axial stress (Figures 14 through 17). Comparison of these models indicated that even at high hydration, the initial energy barrier to the imposed stress was still present for all substituents, suggesting that the stiffness of the substituted forms would be less sensitive to hydration. (This correlation of substituent effects on stiffness is also in

agreement with the observation that substitution decreases the tendency toward the water absorption which causes softening of the polymer.) In general, as with the unsubstituted model, hydration diminished the initial energy barrier found in the energy profiles and shifted the barrier toward lower strain. The nature of the barrier shifted with the type of substitution, but appeared to be more similar to the unsubstituted model with the smaller substituents. The worst departure from the unsubstituted case occurred with phenyl substitution in which the barrier to strain for the axial stress was shifted to far larger strains than in the other cases. This departure may be in agreement with free volume effects by a large group since larger intermolecular distances, and lower intermolecular interaction may lead to larger strains before the build up of an internal resistance to stress. For the perpendicular stress, the only substituent which showed a substantial resistance to the induced strain was the ethyl group. All others showed little or no initial energy barrier to the perpendicular force. These crude models suggest that because of its better insensitivity toward both the stress direction and hydration, the smaller ethyl group may best maintain the mechanical properties of PBI with water content. The models will need to be refined in order to obtain a more quantitative analysis.

The model has also been expanded to a larger system consisting of two strands of an unsubstituted, randomly oriented decamer. The model was generated by initially calculating phi-psi maps of all pertinent dihedral angles, then generating the polymer based upon random distribution of the lowest energy conformations of each dihedral pair (Figure 18). The model was minimized, and hydrated using a 2-angstrom layer (instead of a 5-angstrom layer) in order to keep computation time low. A forcing potential was imposed in the middle of each strand for both the hydrated and unhydrated cases. The energy profiles are shown in Figure 19. The initial slopes which were used to estimate stiffness, drop with increasing hydration (Figure 20). This drop is in agreement with experiment. The trends were not as quantitative as in the trimer case, however the decamer model can also be improved as evidenced in better predictions from a recently refined model (see Figure 20, refined points). In spite of the need for refinement, the decanes case shows the same qualitative trends as the trimers model. The similar trends from both the smaller model and the larger scaled-up system suggests the validity of the trends observed from the trimer model. Newer methods will need to be explored in order to better represent applied strain and temperature for all of the models.

CONCLUSION

Although the modeling technique described is not yet entirely quantitative, by agreement of model trends with experimental, it has demonstrated a method in which to examine individual contributions from different structures, stress orientations, and even rate dependencies to the mechanical response of the polymer. As is shown in this study, contributions from oriented structures are particularly easy to define and study using this technique. Similar methods could eventually be used to increase our understanding of the molecular origins and contributions to mechanical properties such as modulus, break, adhesion, and cohesion. The technique is planned to be extended to better rate determinations and temperature dependencies. It is also planned to be used in studying effects of structure and temperature on modulus, and in quenching studies to predict changes in free volume. The method is also currently being used in a propellant crystal/polymer binder study in order to determine effects of crystalline structure and polymer structure on the mechanical property of the composite material.

REFERENCES

1. Biosym Technologies, Inc. "Discover User Guide, Part 1," Version 2.8, 1992.

2. Alan Buckley, D. E. Stuetz, and G. A. Serad. "Polybenzimidazoles," *Encyclopedia of Polymer Science and Engineering*, Vol. 11. John Wiley & Sons, 1988, pp. 512-601.

3. Leo R. Belohlav. "Polybenzimidazole," *Die Angewandte Makromolekulare Chemie*, **40/41** (1974), pp. 465-483.

4. Joseph R. Leal. "Polybenzimidazoles," *Modern Plastics*, August 1975, pp. 60-62.

5. Gaetano Guerra, Soonja Choe, David J. Williams, Frank E. Karasz, and William J. MacKnight. "Fourier Transform Infrared Spectroscopy of Some Miscible Polybenzimidazole/Polyimide Blends," *Macromolecule*, Vol. 21 (1988), pp. 231-234.

6. P. Musto, F. E. Karasz, and W.J. MacKnight. "Hydrogen Bonding in Polybenzimidazole/Polyimide Systems: A Fourier-Transform Infra-red Investigation Using Low-Molecular Weight Monofunctional Probes," *Polymer*, Vol. 30 (1989), pp. 1010-1021.

7. Eberhard W. Neuse and Mohamed S. Loonat. "Two Stage Synthesis via Poly(azomethine) Intermediates," *Macromolecules*, Vol. 16 (1983), pp. 128-136.

8. N. Iwamoto and R. Yee. "Modeling of Water Absorption by Polybenzimidazole," presented at the Second Annual R&D Information Exchange Conference, Naval Weapons Center, China Lake, Calif., 2-4 April 1991.

9. N. Iwamoto. "PBI Hydration Study in the Development of Methodology for the Molecular Modeling of Mechanical Property Trends," presented at the 1991 U.S. Army Chemical Research, Development, and Engineering Center Scientific Conference; Aberdeen Proving Ground, Maryland, 19-22 November 1991.

10. Caibao Qian and P. J. Ludovice, "Stress/Strain Analysis of Polymeric Materials by Molecular Dynamics Simulations," *Polym. Preprints*, **33**, 1992, 623-624.

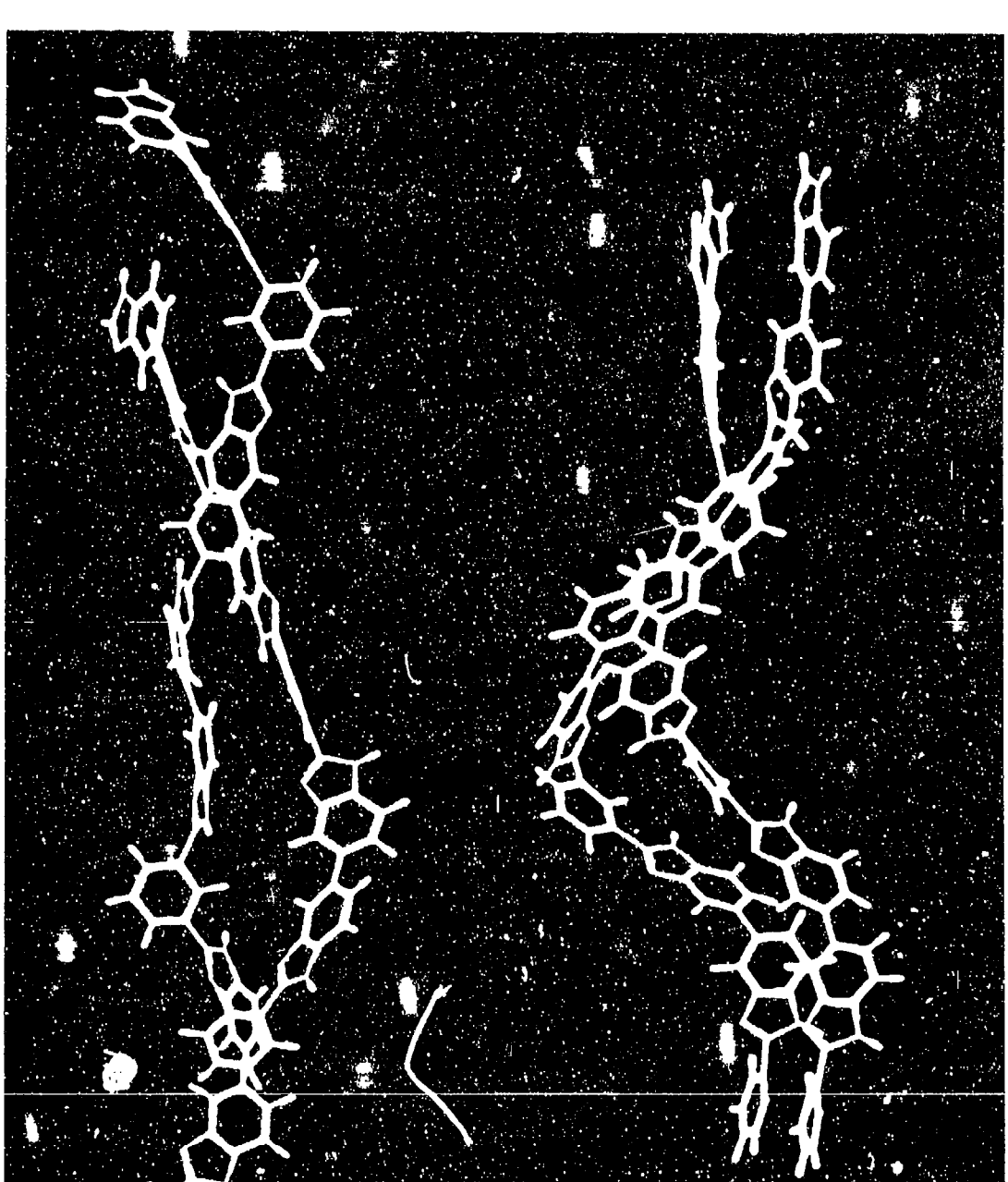

FIGURE 1. ~~Top~~: Minimized Unhydrated Trimer Model. ~~Bottom~~: Trimer Model After Application of Axial Strain.
Top
Bottom

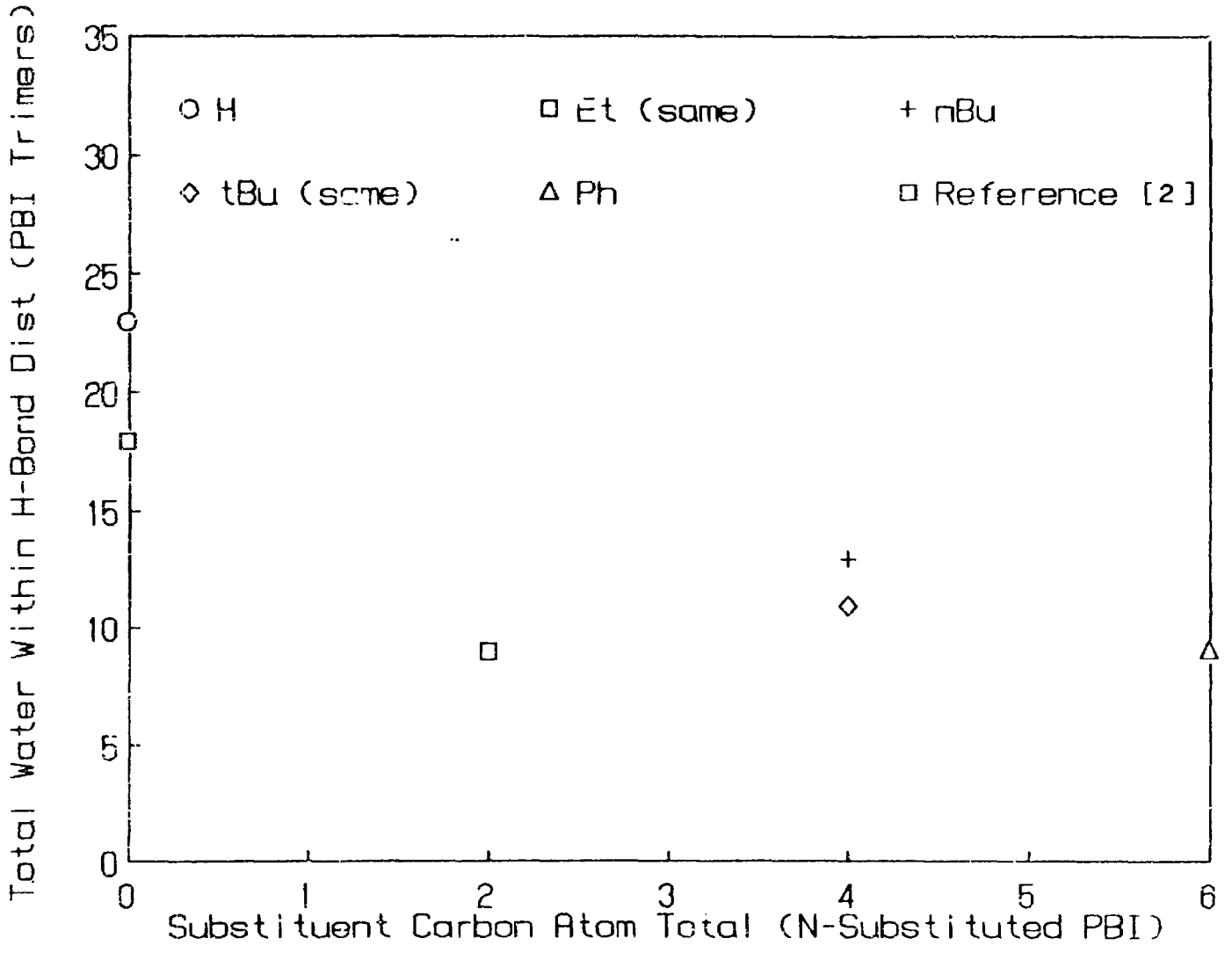

FIGURE 2. Substituent Effect on Hydrogen-Bonded Water. (Total number of water molecules vs. total number of carbon atoms in substituent.)

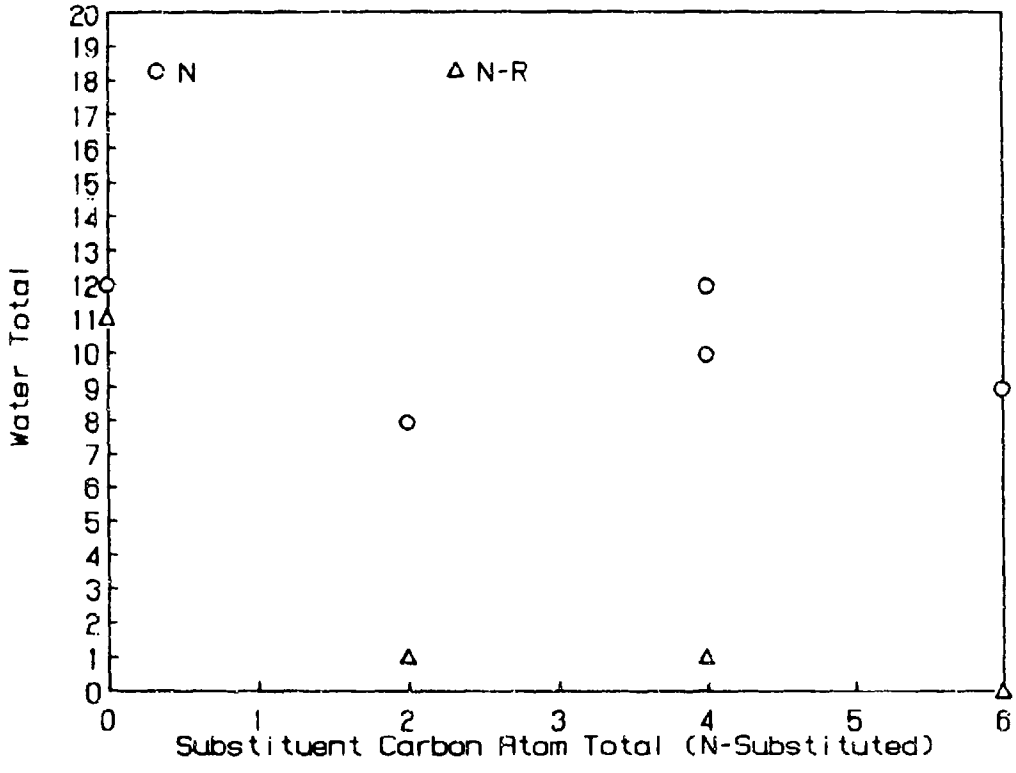

FIGURE 3. Effect of Nitrogen Type and Substituent on Hydrogen-Bonded Water. (Total number of water molecules vs. total number of carbon atoms in substituent.)

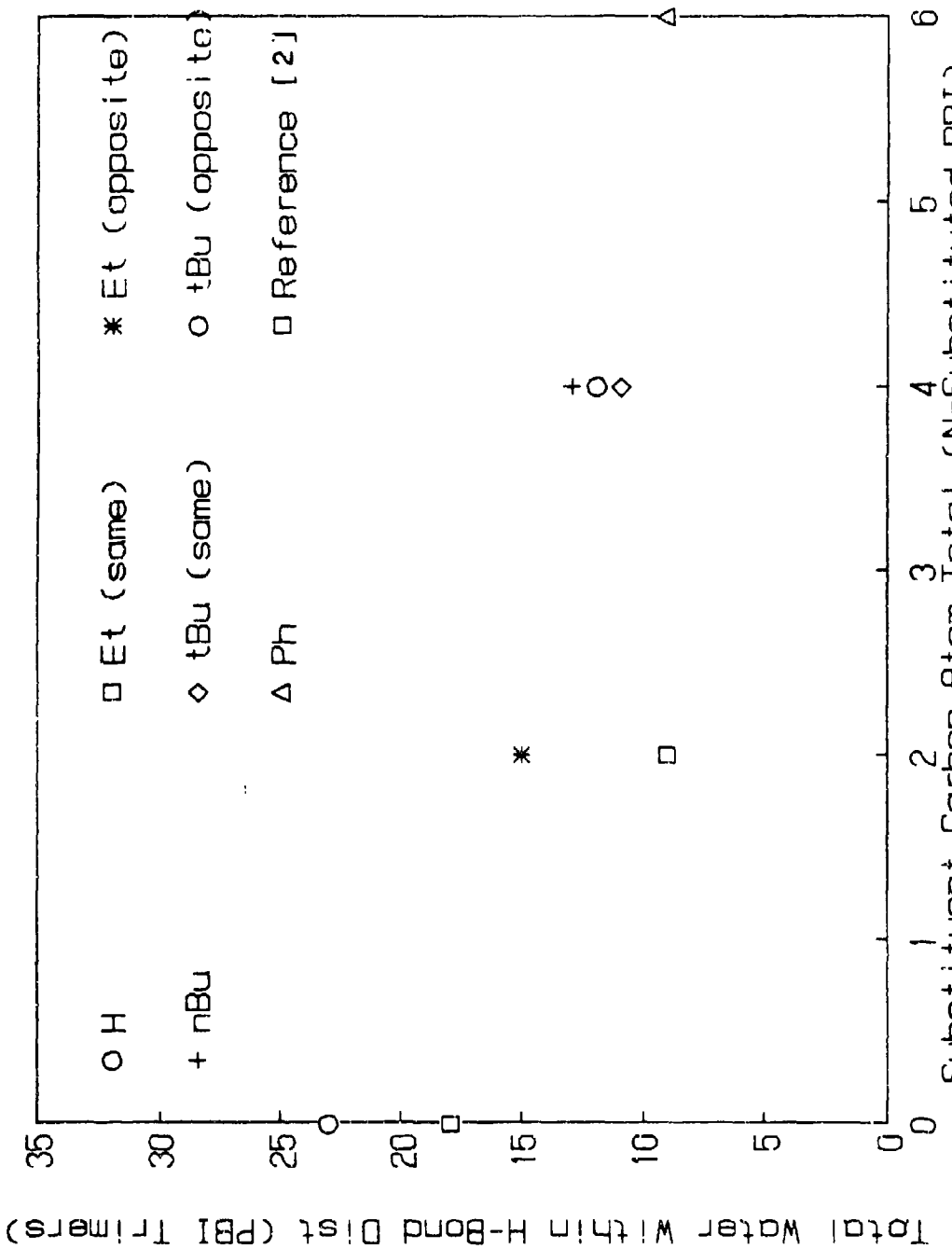

FIGURE 4. Effect of Substituent Regiochemistry on *Hydrogen-Bonded Water*
(Same = substituents on same sides; Opp = substituents on opposite sides). (Total number of water molecules *vs.* total number of carbon atoms in substituent.)

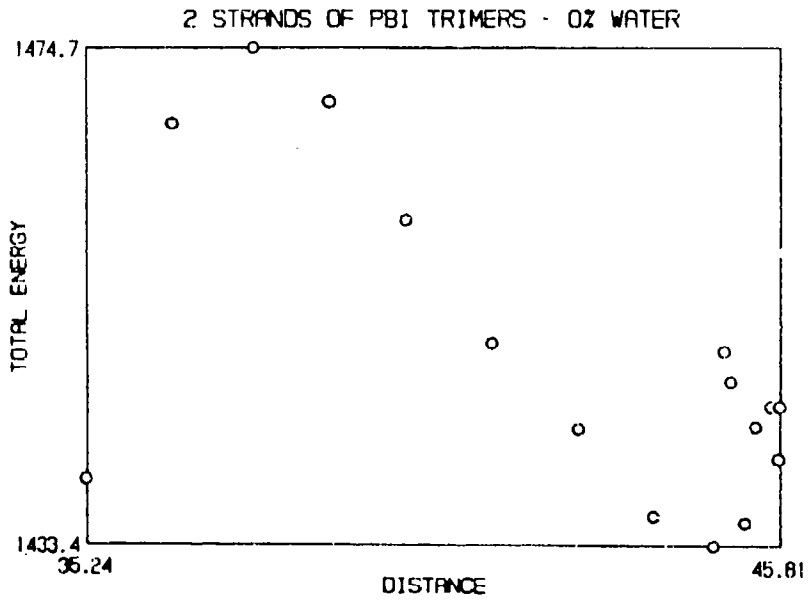

(a)

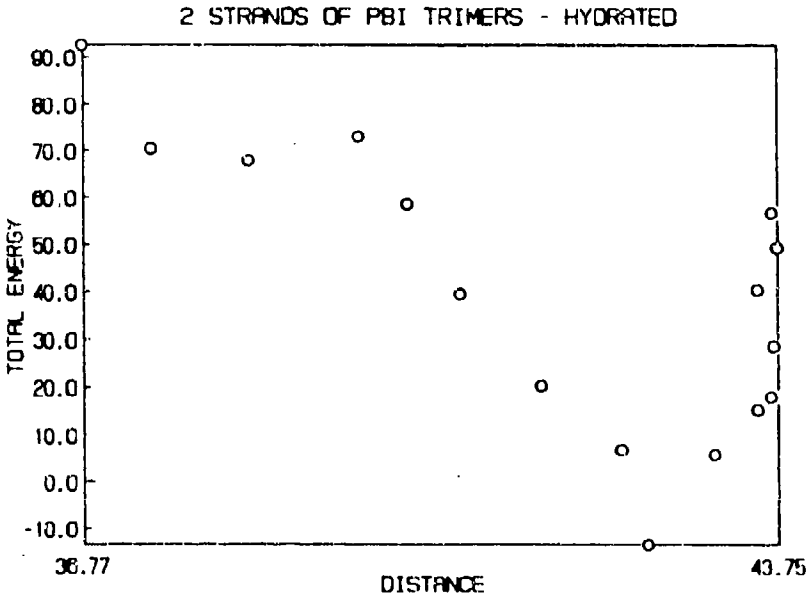

(b)

FIGURE 5. Effect of Hydration on Trimer Energy Profiles Using an Axial Stress: (a) Unhydrated (unsubstituted) and (b) Hydrated (unsubstituted). (Kcal vs. angstroms.)

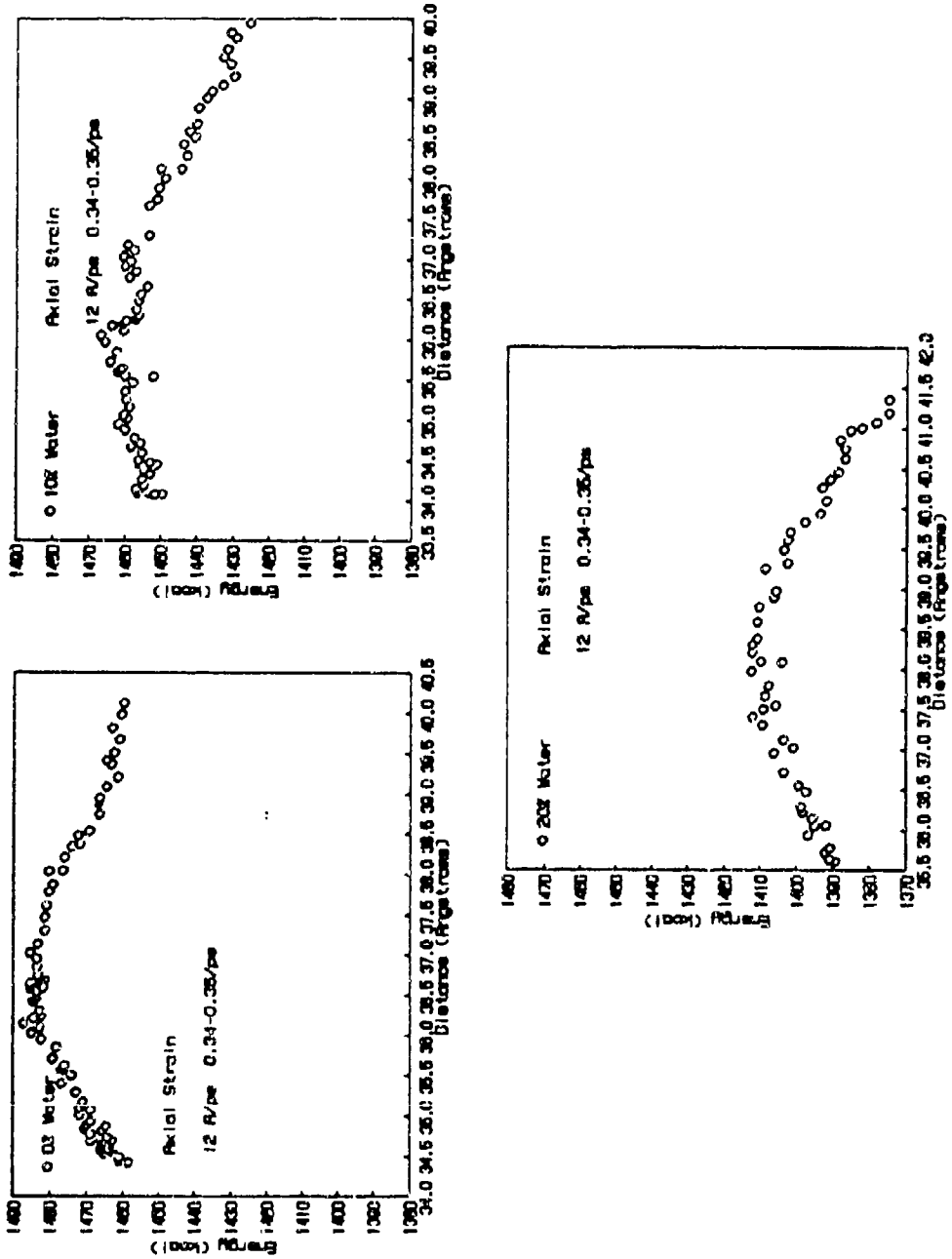

FIGURE 6. Refined Trimer Model Showing Effect of Hydration on Energy Profiles Using an Axial Stress at 0, 10, and 20% Water (unsubsituted).

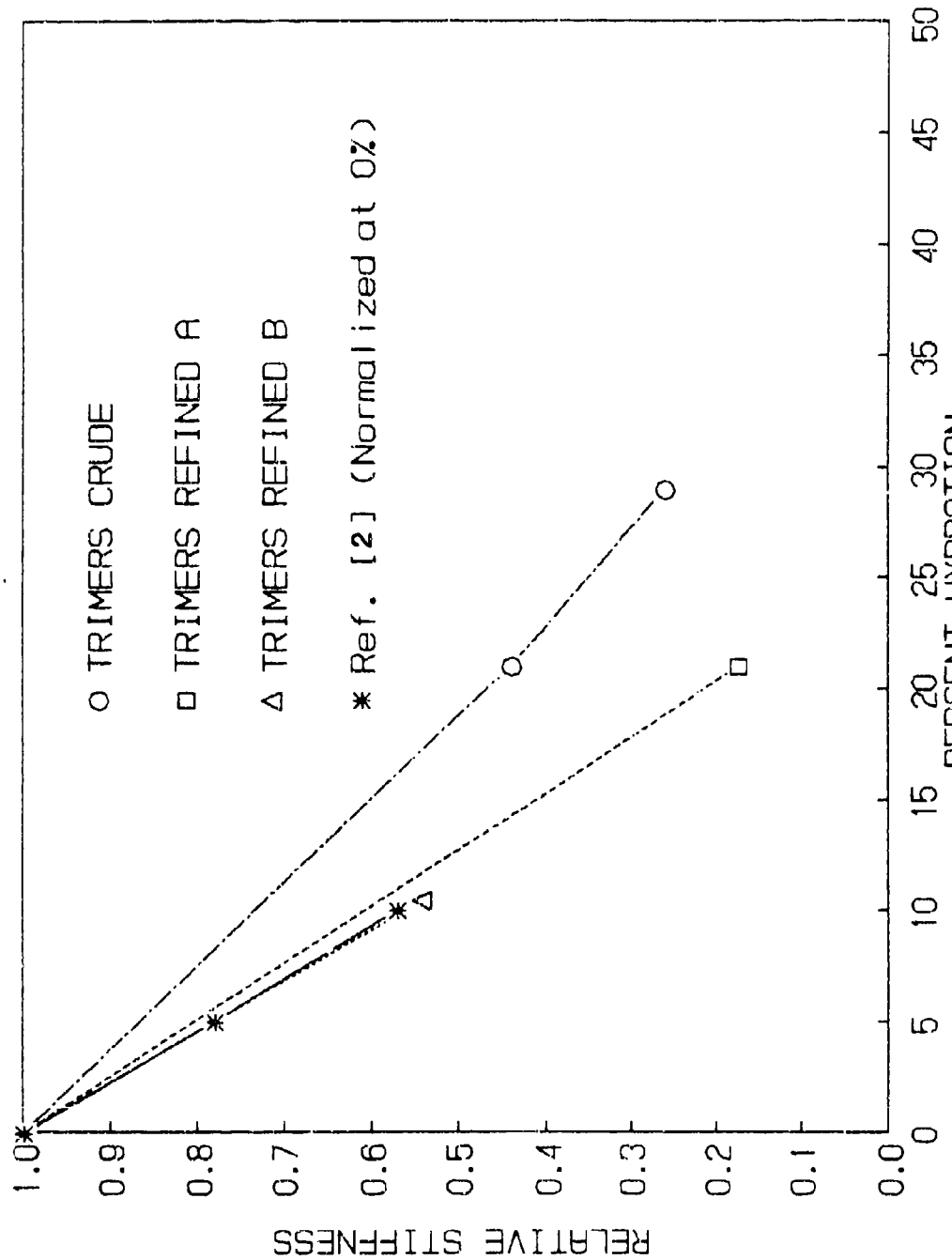

FIGURE 7. Effect of Hydration on Stiffness Trends.

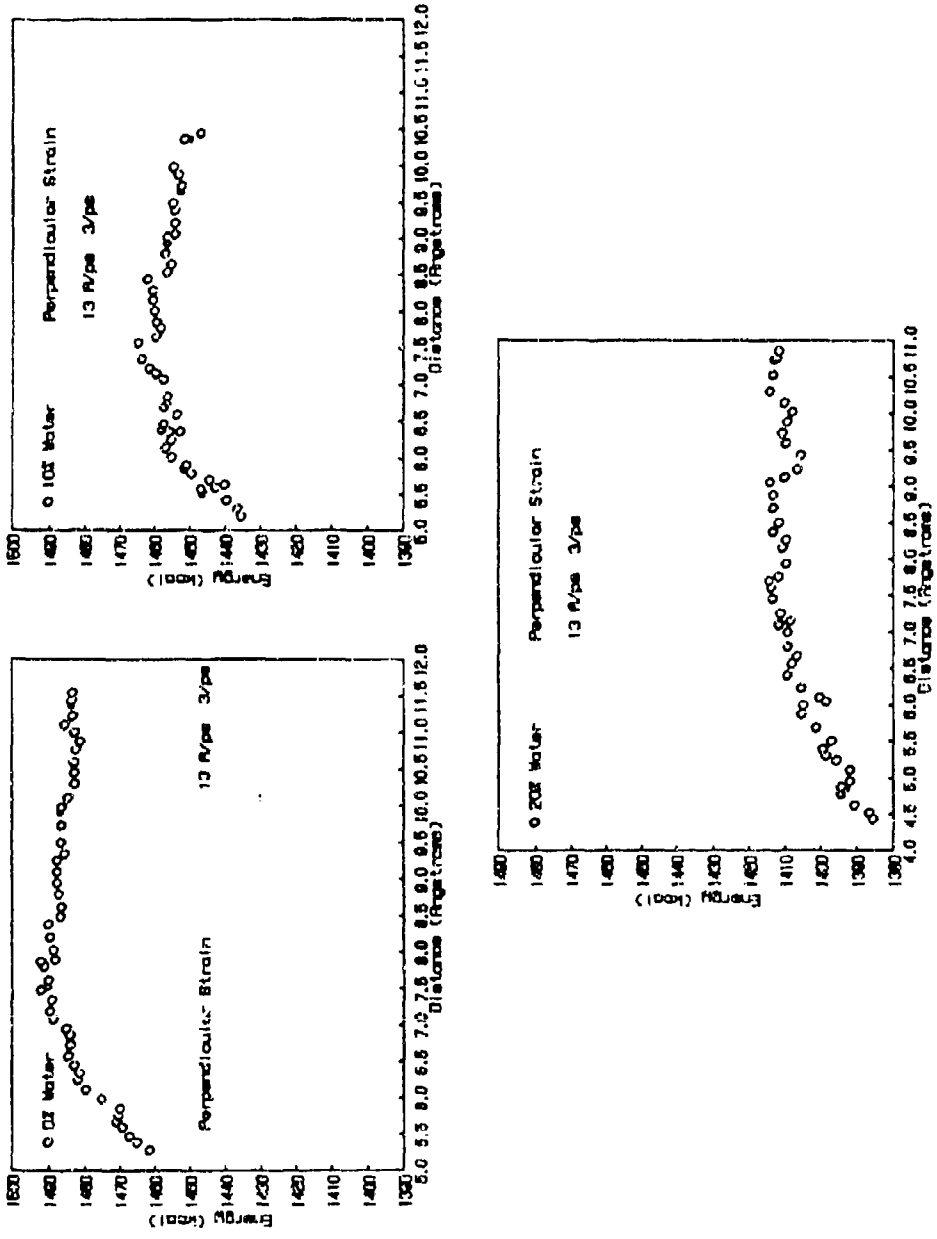

FIGURE 8. Effect of Hydration on Trimer Energy Profiles Using a Perpendicular Stress at 2.5-3.0 ps^{-1} at 0, 10, and 20% Water (unsubstituted).

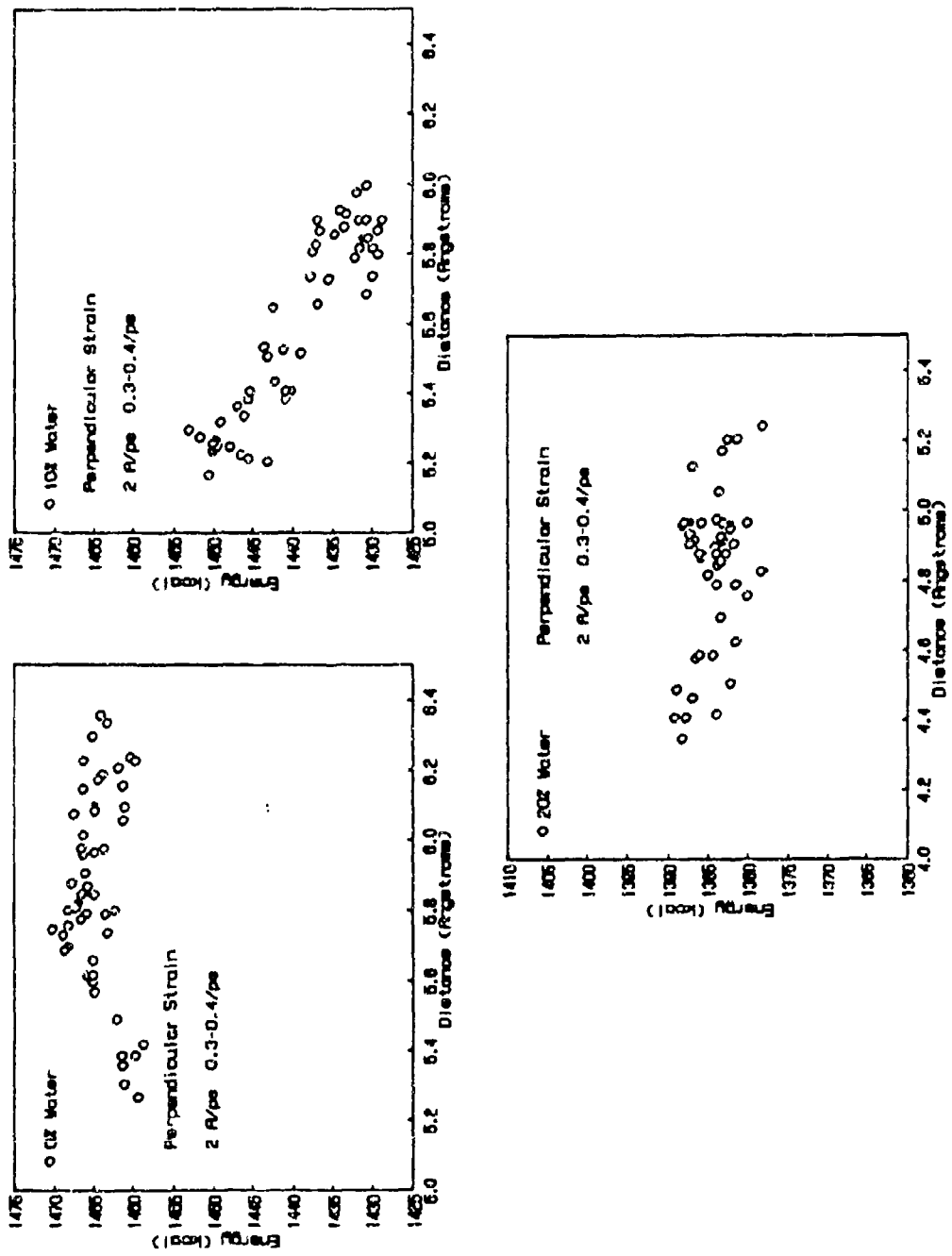

FIGURE 9. Effect of Hydration on Trimer Energy Profiles Using a Perpendicular Stress at 0.3-0.4 ps^{-1} at 0, 10, and 20% Water (unsubstituted).

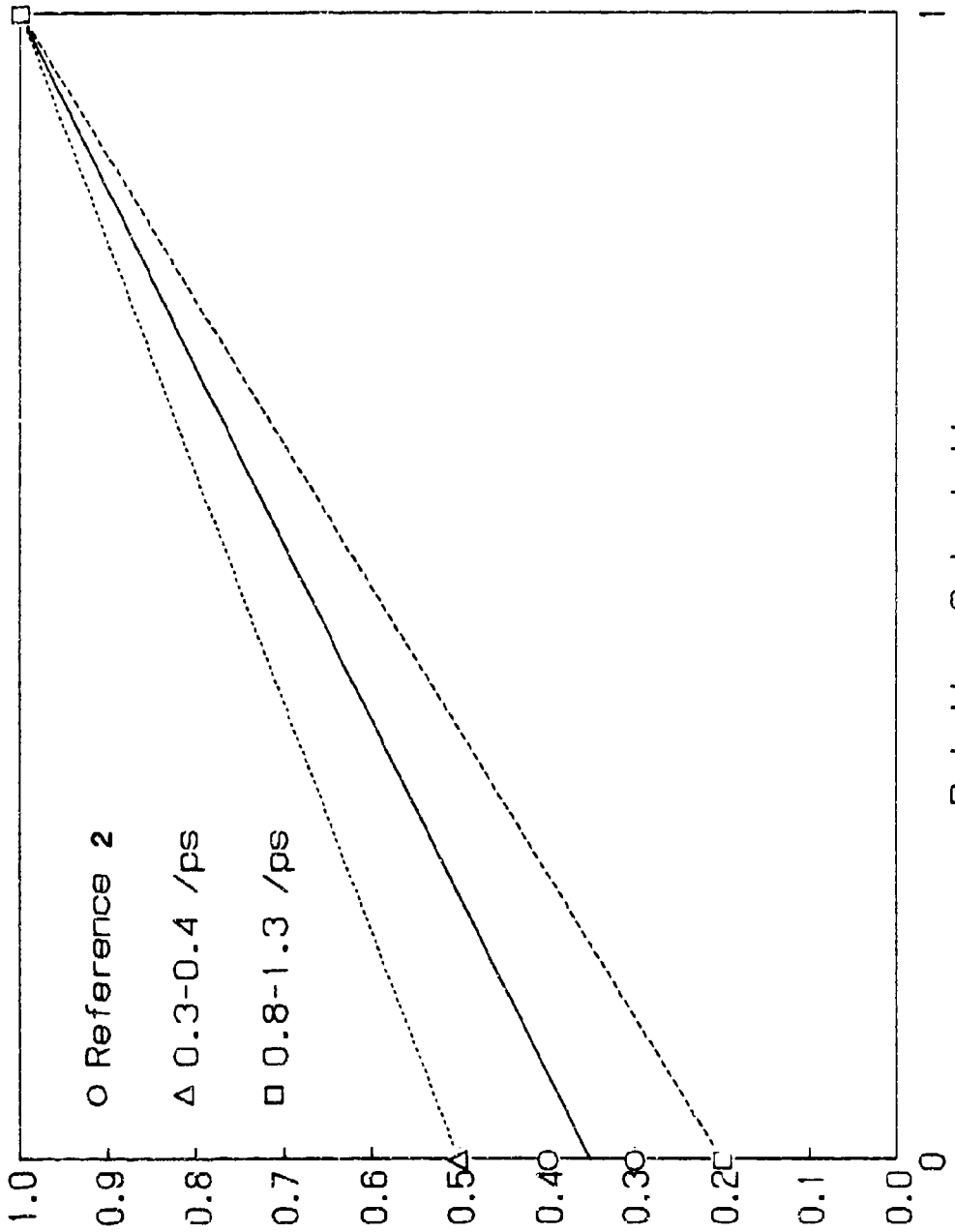

FIGURE 10. Effect of Orientation on Relative Stiffness (0 = undrawn or perpendicular stress and 1 = drawn or axial stress).

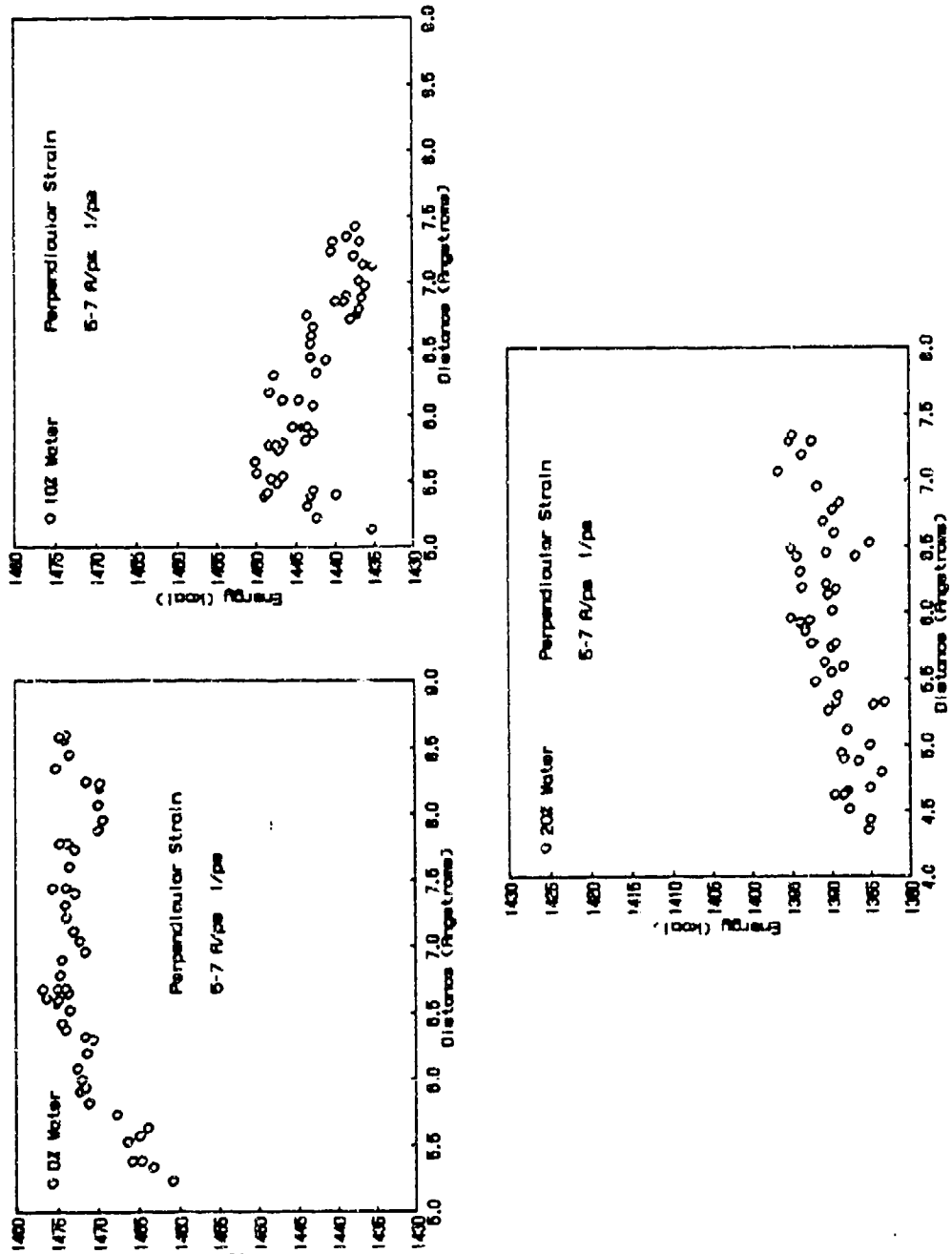

FIGURE 11. Effect of Hydration on Trimer Energy Profiles Using a Perpendicular Stress at 1.0-1.2 ps^{-1} at 0, 10, or 20% Water (unsubstituted).

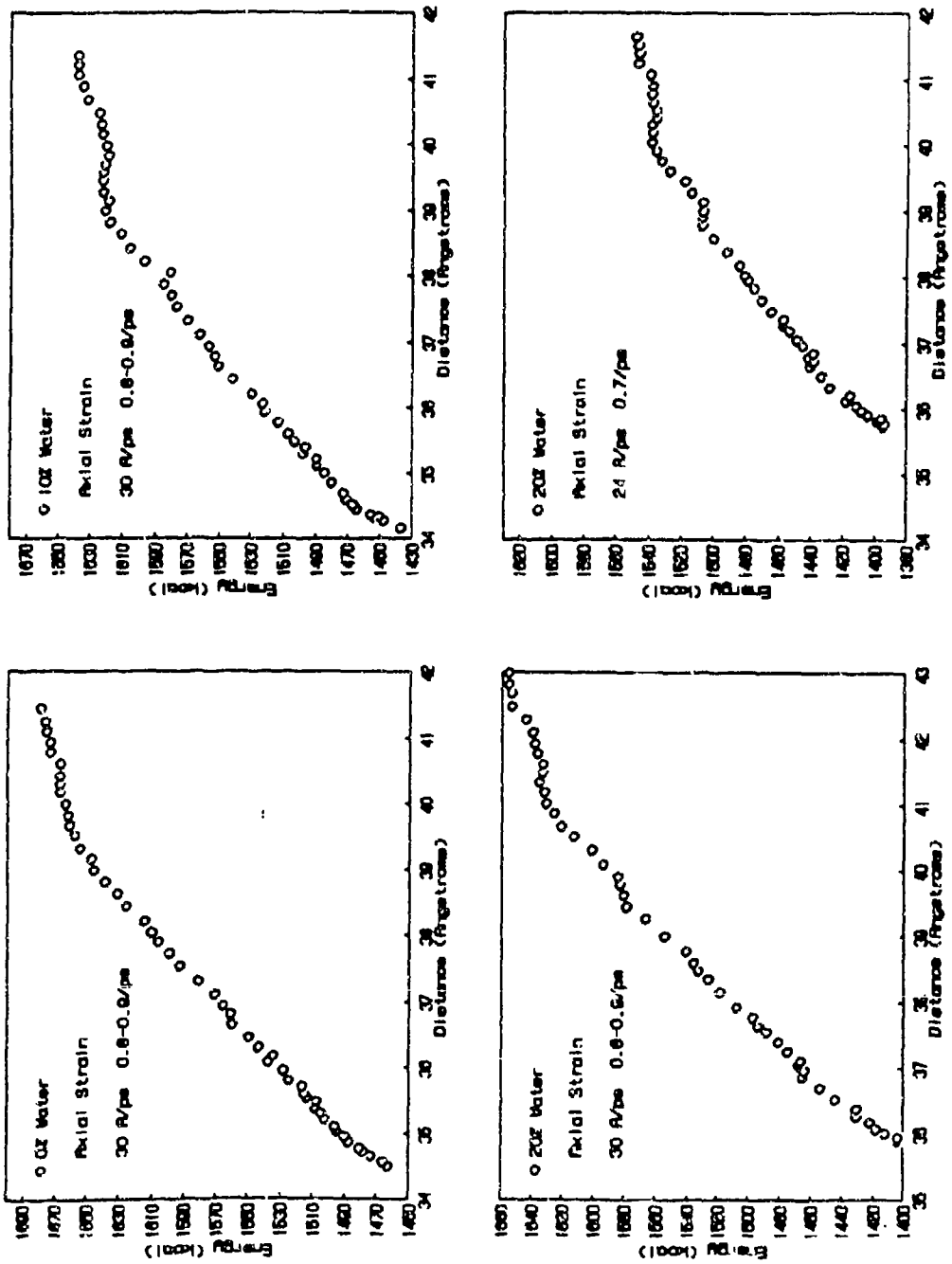

FIGURE 12. Effect of Hydration on Trimer Energy Profiles Using a High-Rate Axial Stress at 0, 10, and 20% Water (unsubstituted).

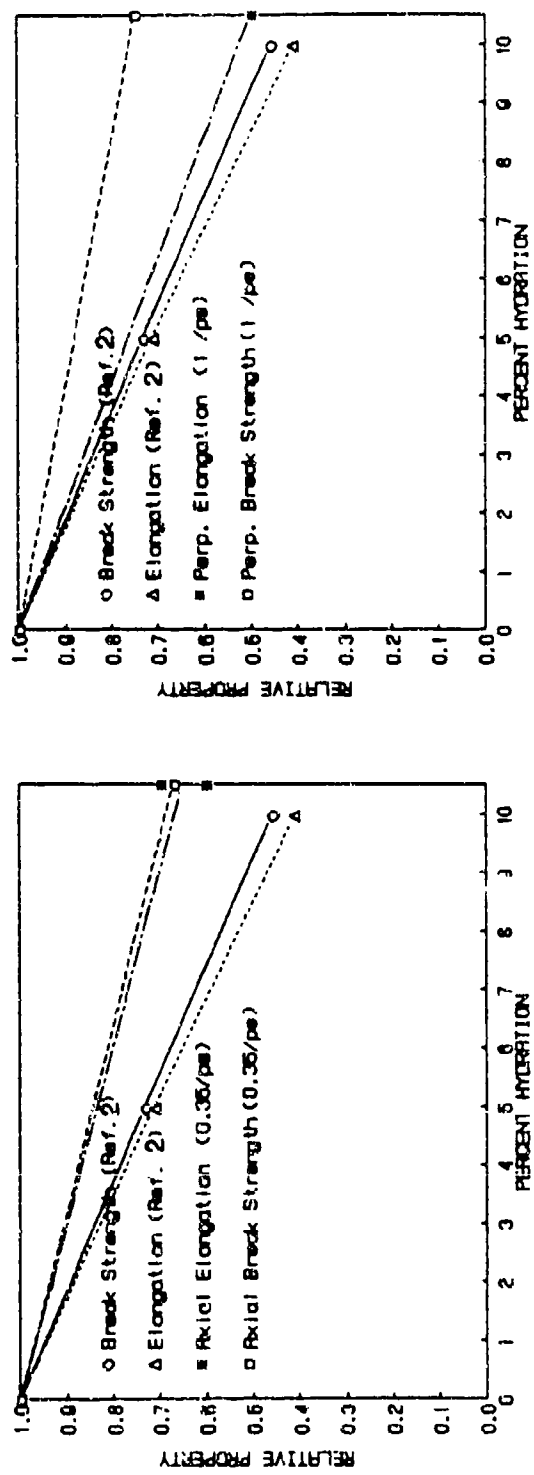

FIGURE 13. Effect of Hydration on Strength and Strain-to-Break Trends.

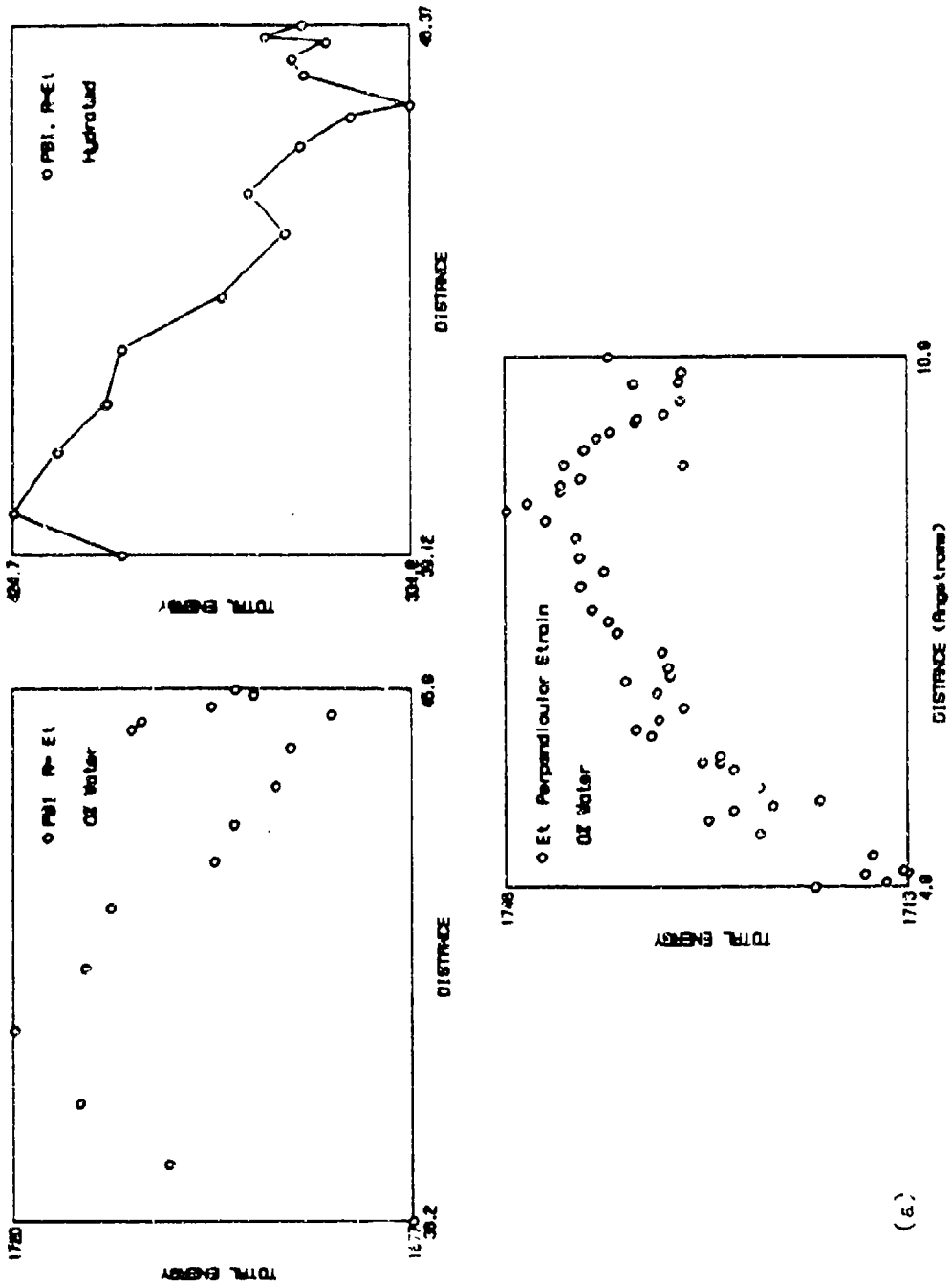

FIGURE 14. Effect of Hydration in Ethyl Substituted Trimers; (a) Substitution on Same Sides and (b) Substitution on Opposite Sides. (Kcal vs. angstroms.)

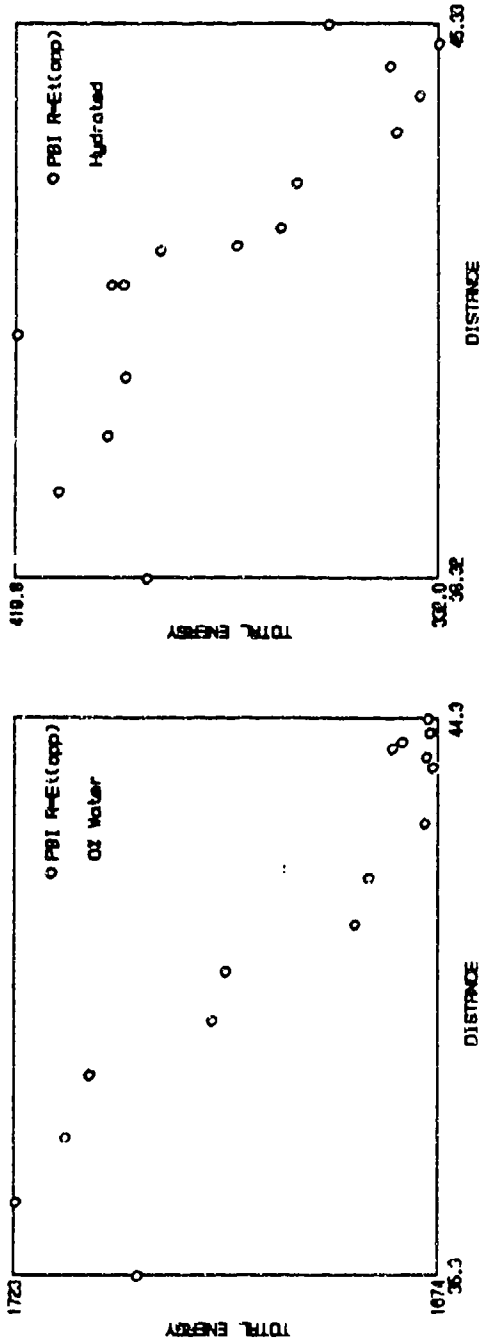

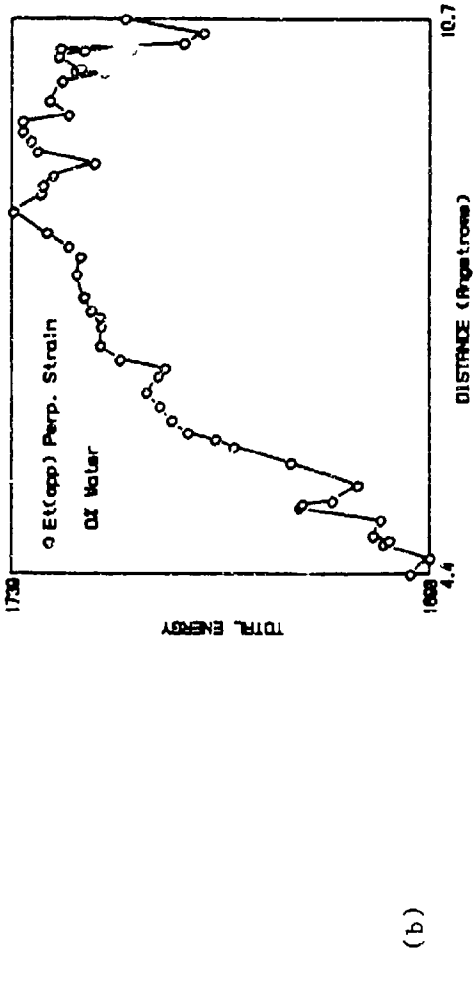

(b)

FIGURE 14. (Continued) Effect of Hydration in Ethyl Substituted Trimers: (a) Substitution on Same Sides and (b) Substitution on Opposite Sides. (Kcal vs. angstroms.)

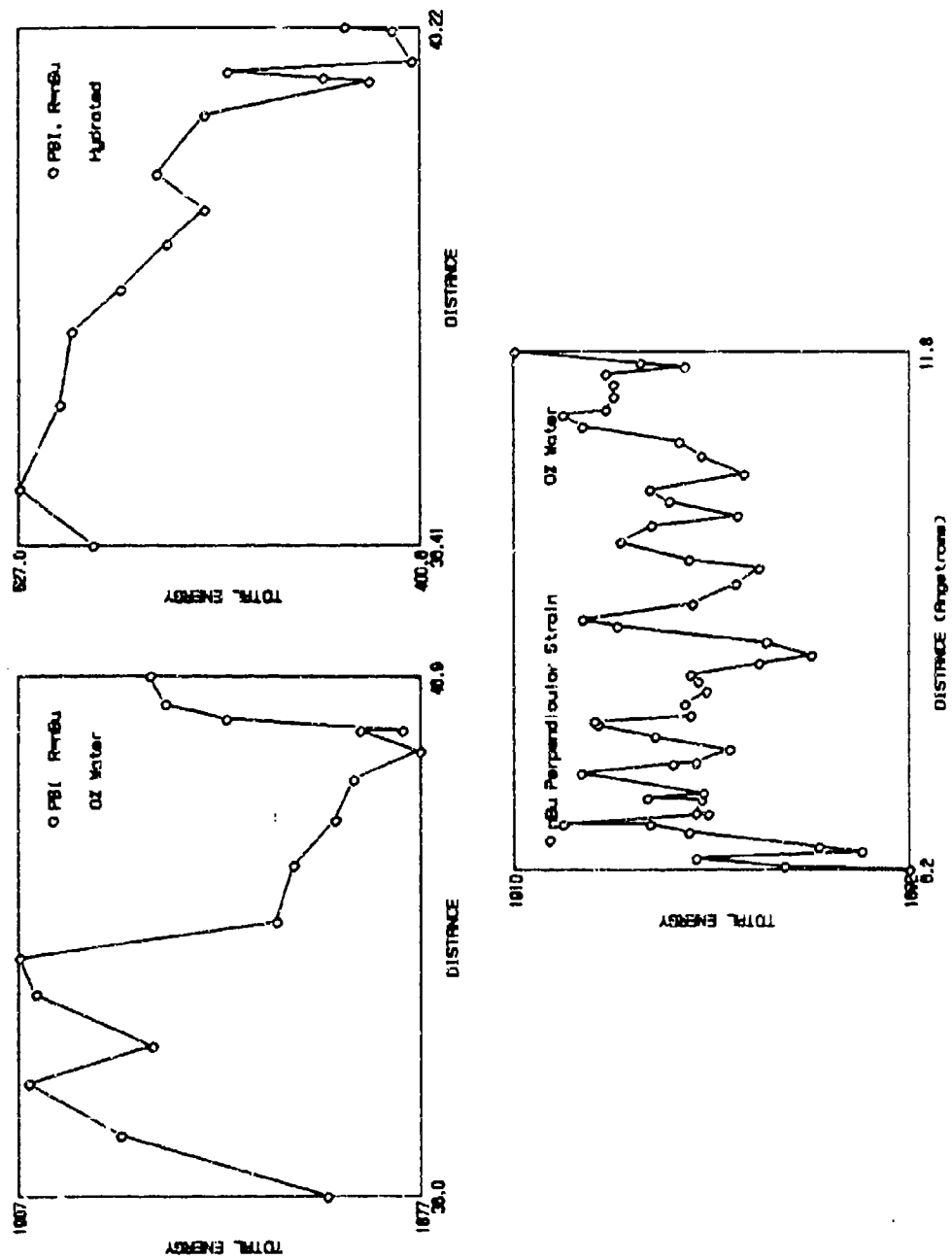

FIGURE 15. Effect of Hydration in n-Butyl Substituted Trimers. (Kcal vs. angstroms.)

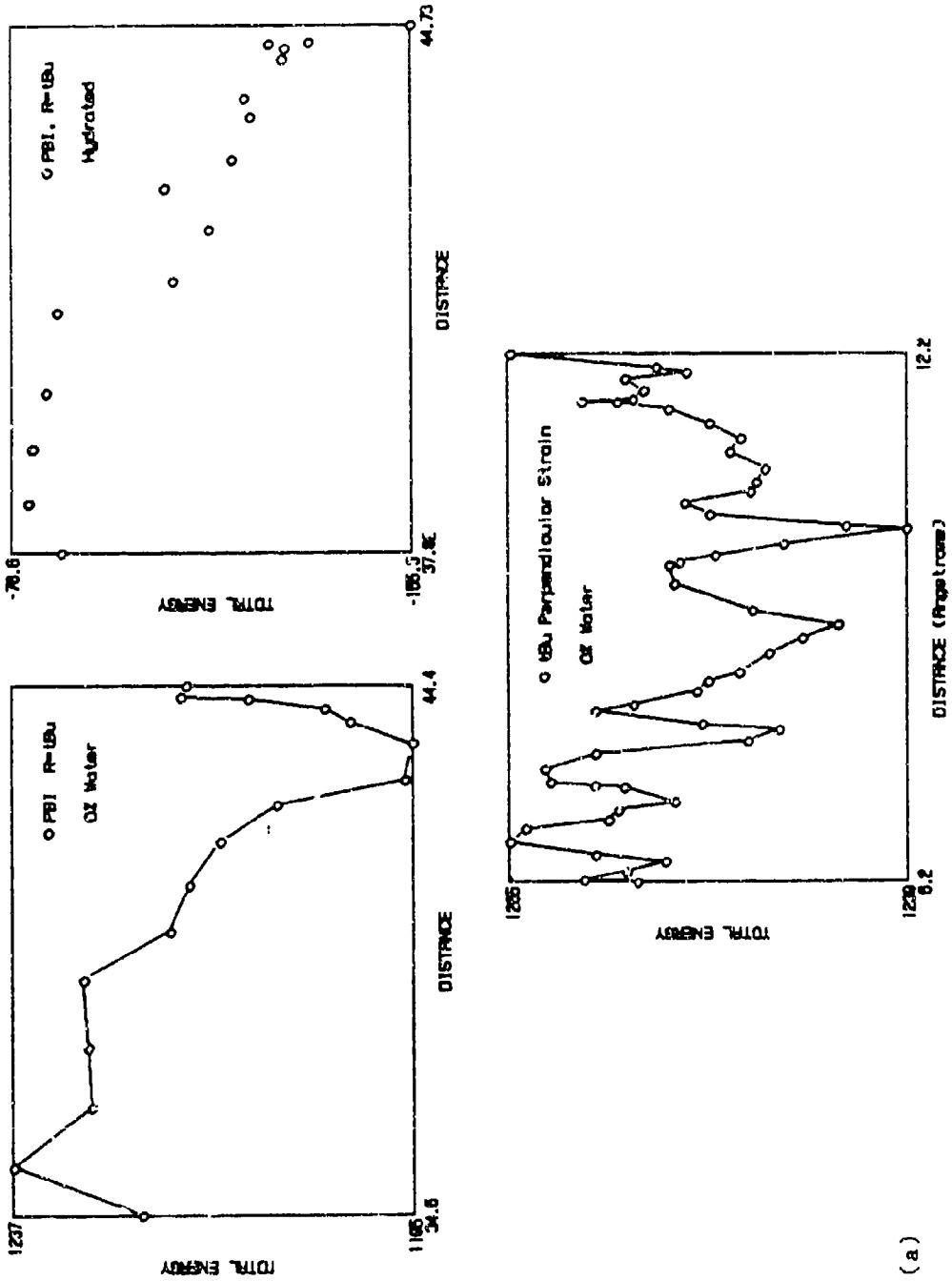

FIGURE 16. Effect of Hydration in t-Butyl Substituted Trimers: (a) Substitution on Same Sides; (b) Substitution on Opposite Sides. (Kcal vs. angstroms.)

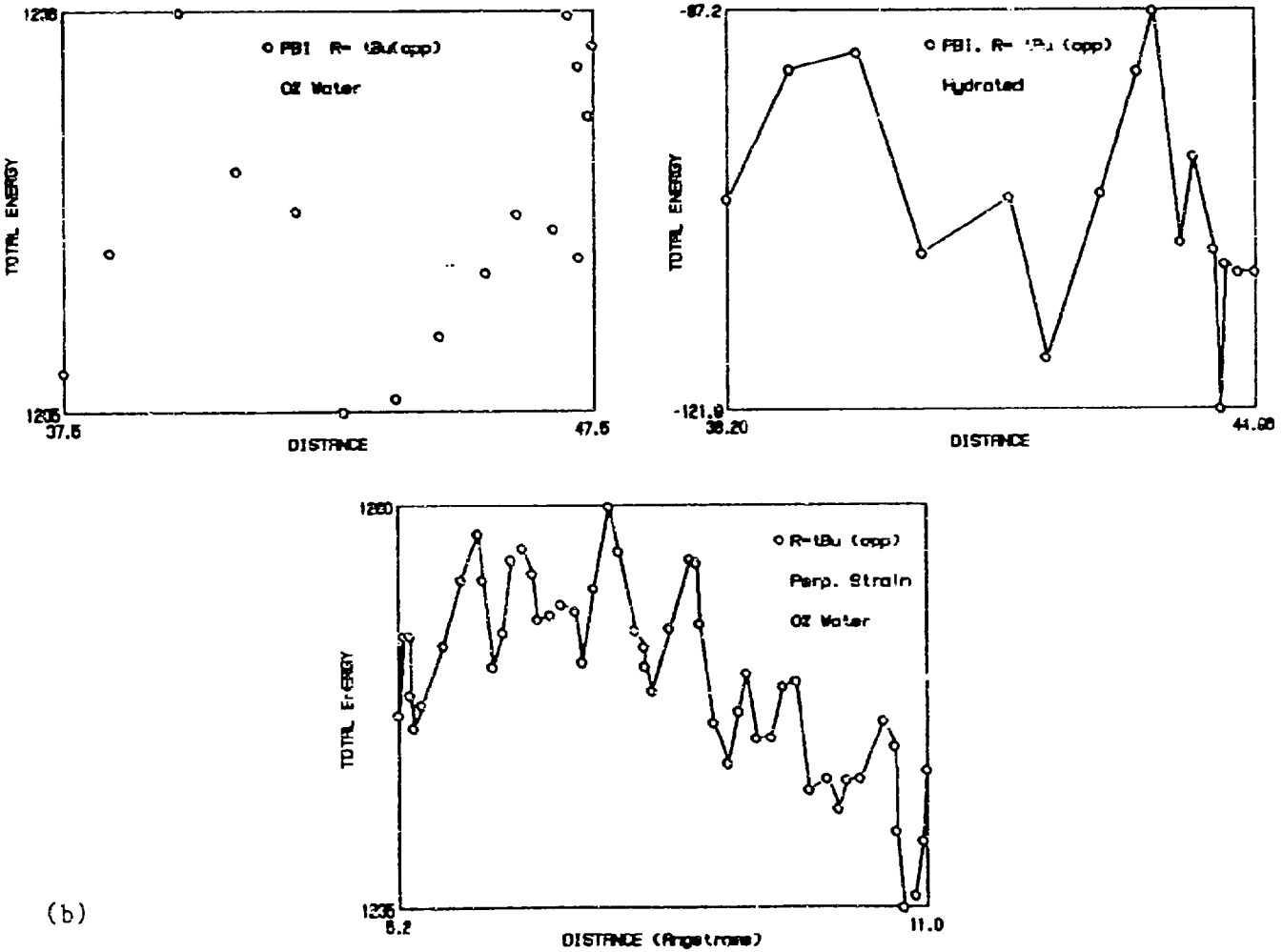

(b)

FIGURE 16. (Continued) Effect of Hydration in t-Butyl Substituted Trimers: (a) Substitution on Same Sides, (b) Substitution on Opposite Sides. (K .l vs. angstroms.)

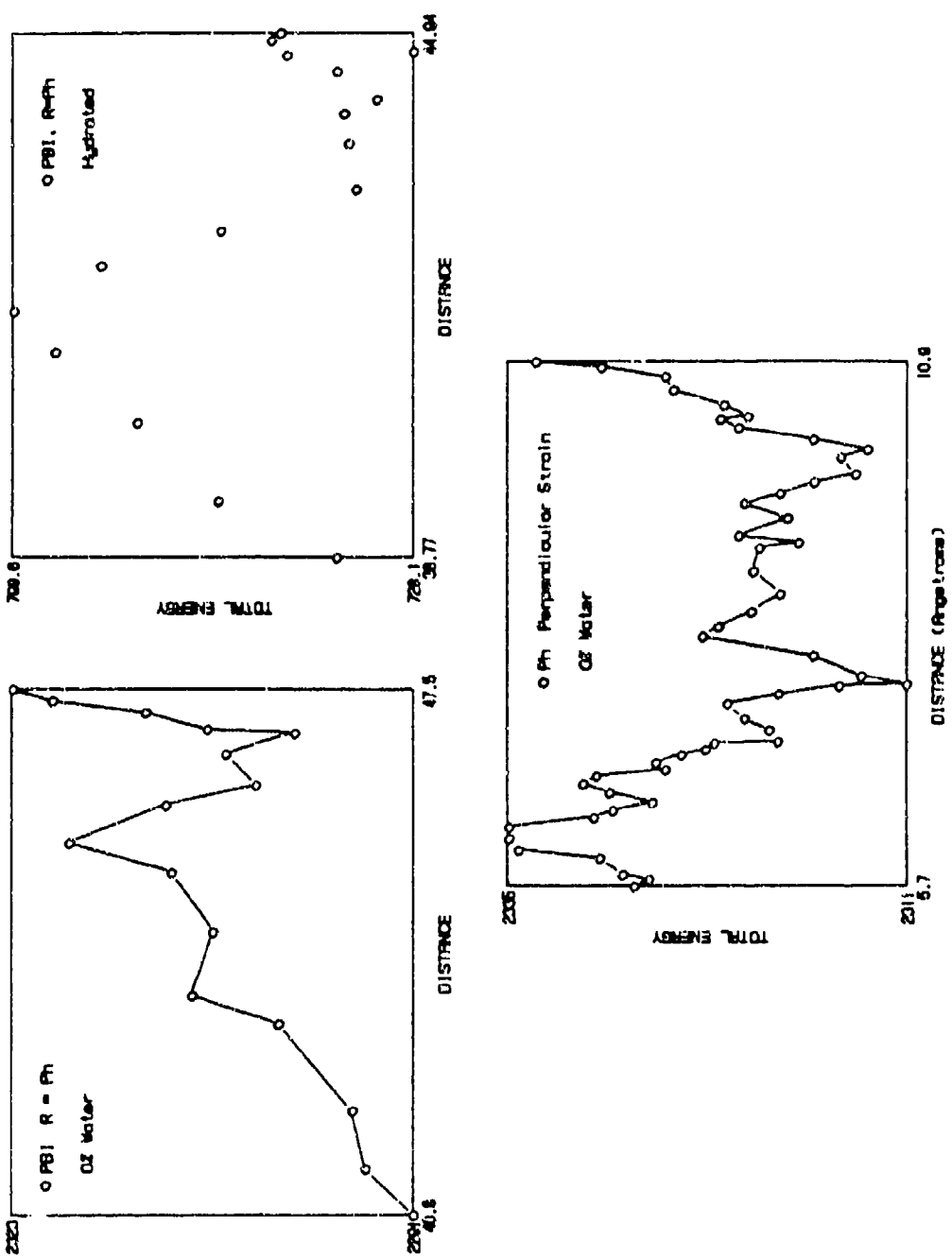

FIGURE 17. Effect of Hydration in Phenyl Substituted Trimers. (Kcal vs. angstroms.)

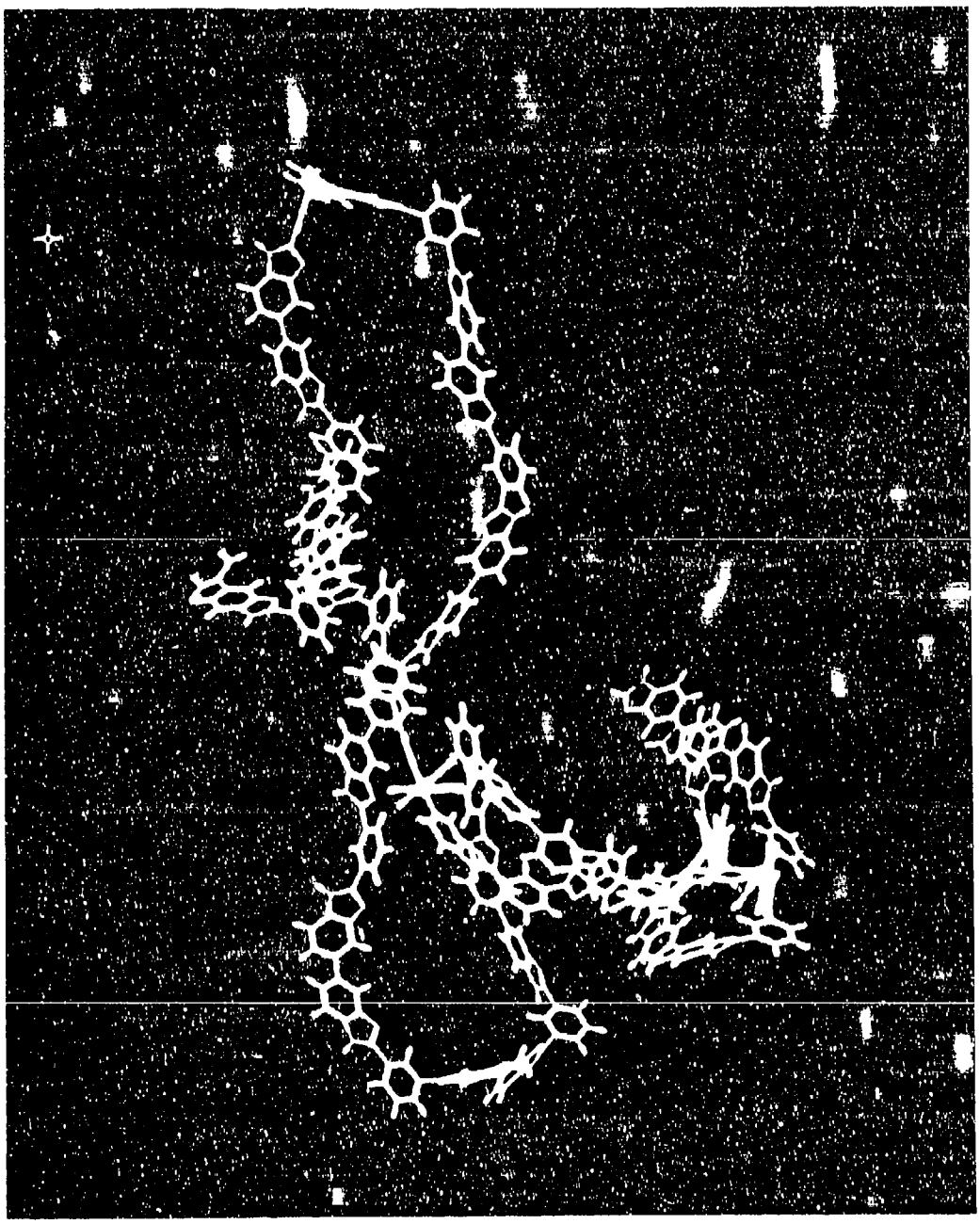

FIGURE 18. Unhydrated Decamer Model.

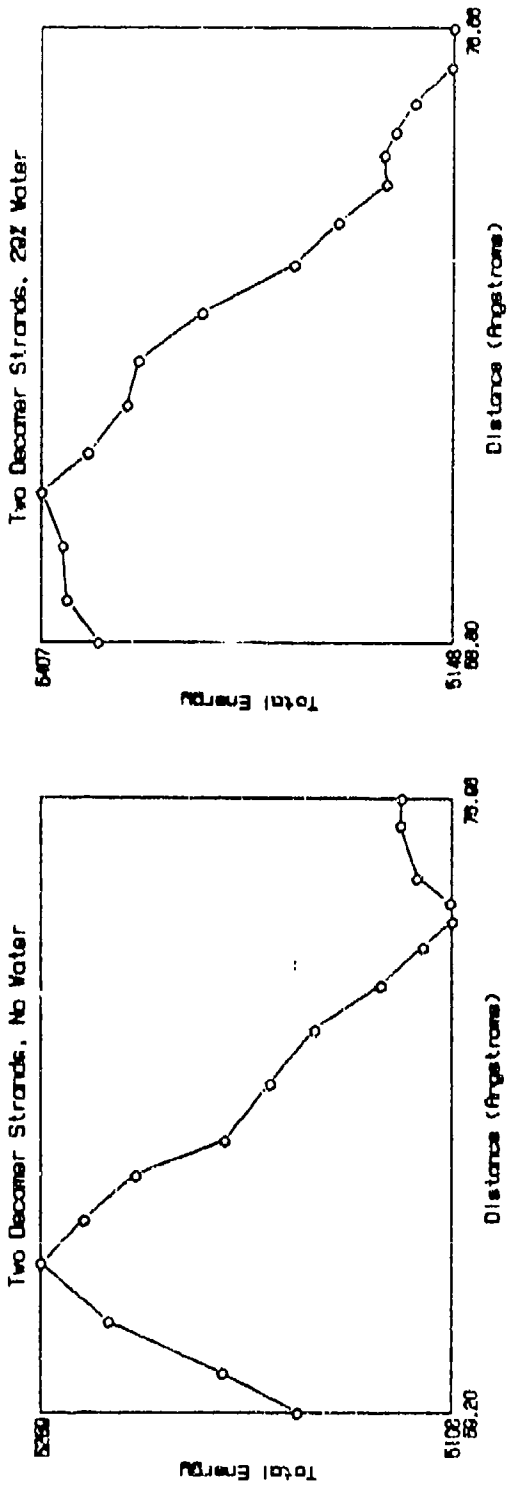

FIGURE 19. Effect of Hydration on Decamer Energy Profiles. (Kcal vs. angstroms.)

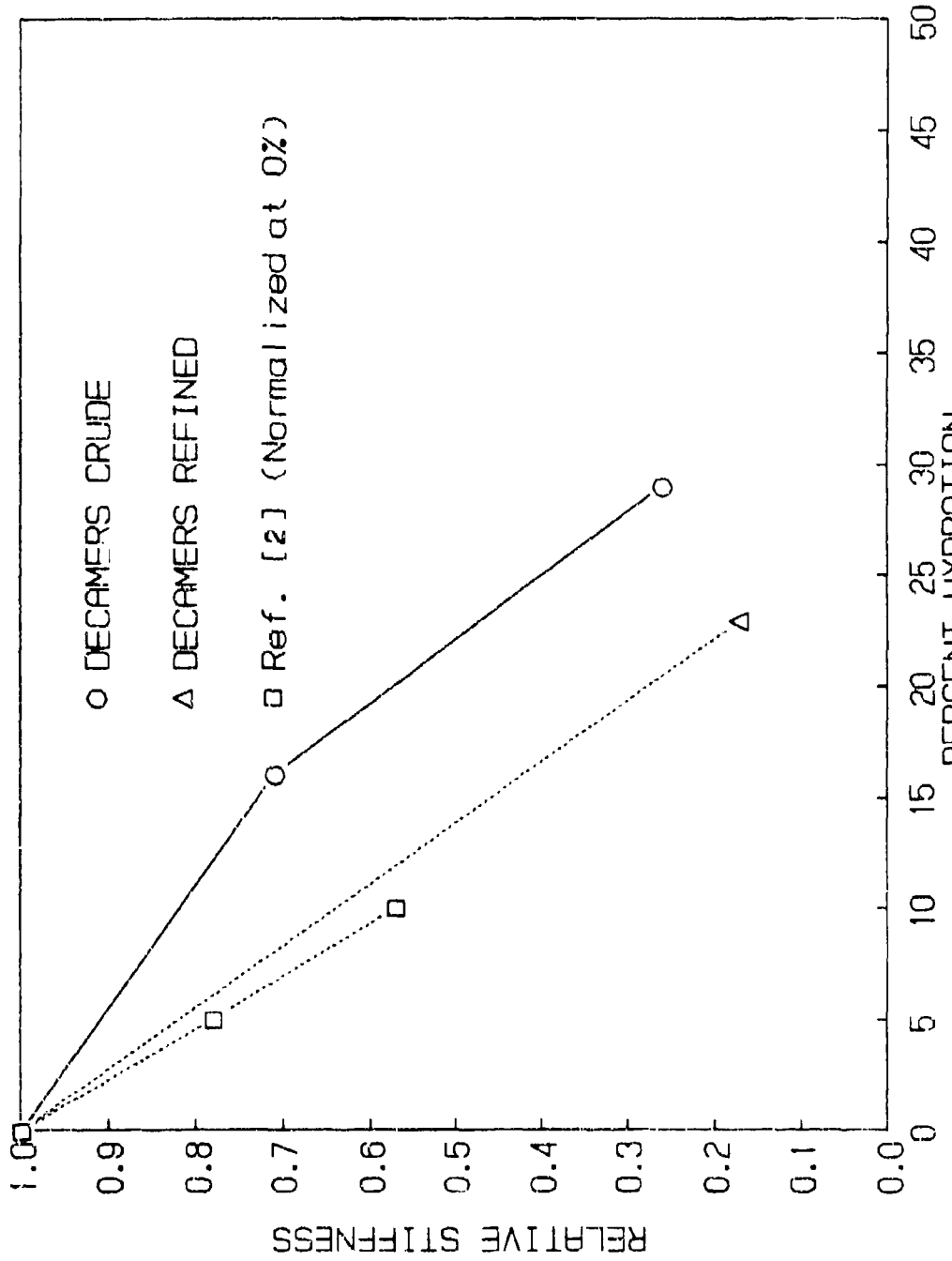

FIGURE 20. Effect of Hydration on Stiffness in the Decamer Model.

INITIAL DISTRIBUTION

1 Commander in Chief, U. S. Pacific Fleet, Pearl Harbor (Code 325)
1 Commander, Third Fleet
1 Commander, Seventh Fleet
2 Naval Academy, Annapolis (Director of Research)
1 Naval War College, Newport
1 Army Chemical Research, Development and Engineering Center, Aberdeen Proving Ground (SMCCR-RSP-C, Dr. A. Harper)
1 Army Research, Development and Engineering Center, Natick (STRNC-YSM, J. Walker)
1 Air Force Intelligence Agency, Bolling Air Force Base (AFIA/INT, MAJ R. Esaw)
1 Wright Laboratory/Dynamics Laboratory, Wright-Patterson Air Force Base (WL/MLPJ, Hardened Materials Branch, R.Pachter)
2 Defense Technical Information Center, Alexandria
1 Hudson Institute, Incorporated, Center for Naval Analyses, Alexandria, VA (Technical Library)